

## Determination of $L$ -shell X-ray production cross-sections in holmium by 10–40 keV photons

K S MANN, K S KAHLON, H S AULAKH, N SINGH, R MITTAL,  
K L ALLAWADHI and B S SOOD

Nuclear Science Laboratories, Physics Department, Punjabi University, Patiala 147002,  
India

MS received 16 June 1990; revised 7 June 1991

**Abstract.** In an effort to resolve the existing discrepancy between experiment and theory, the cross-sections for the production of  $L_1$ ,  $L_\alpha$ ,  $L_\beta$  and  $L_\gamma$  groups of  $L$ -shell X-rays of Ho by photons of nine energies in the range 10–40 keV have been measured using an improved version of annular source double reflection geometrical set-up. Contrary to the earlier findings of Garg *et al* that the measured values of the cross-sections are consistently higher than those calculated theoretically, the present results do not confirm this. The plausible deficiencies in the experiments of Garg *et al* are pointed out and possible remedies to overcome them are suggested. It is concluded that the higher values obtained by Garg *et al* are probably due to systematic errors in their method of measurement.

**Keywords.**  $L$ -shell; fluorescent X-rays; production cross-sections.

PACS No. 32-80

### 1. Introduction

An improved annular source double reflection experimental set-up and method of measurement for the determination of  $L$ -shell X-ray fluorescence cross-section which takes care of the systematic errors due to the deficiencies in the previous measurements of Garg *et al* (1986) have been used to measure the cross-sections for the production of  $L_1$ ,  $L_\alpha$ ,  $L_\beta$  and  $L_\gamma$  X-rays in Ho by the K conversion X-rays of Ge, Se, Rb, Zr, Mo, Ag, Sn, Ba and Nd corresponding to weighted mean energies of 10.005, 11.372, 13.596, 16.035, 17.781, 22.581, 25.77, 32.89 and 38.189 keV respectively. Contrary to the findings of Garg *et al* (1986) that the experimental values are consistently higher than the calculated values, our results do not confirm this. The deficiencies in the previous set-up and method of measurement are pointed out. The new set-up and method of measurement are described. The results alongwith the reasons for the reported discrepancy are discussed.

### 2. Experimental procedure and method of measurement

The experimental arrangements used by us and by Garg *et al* (1986) are shown in figures 1(a) and 1(b) respectively. Primary targets (P) of thickness ranging from 13 to 350 mg/cm<sup>2</sup> of elements mentioned above are irradiated, in turn, with 59.57 keV gamma rays from an annular radioactive source (R) of <sup>241</sup>Am with strength 1 Ci and

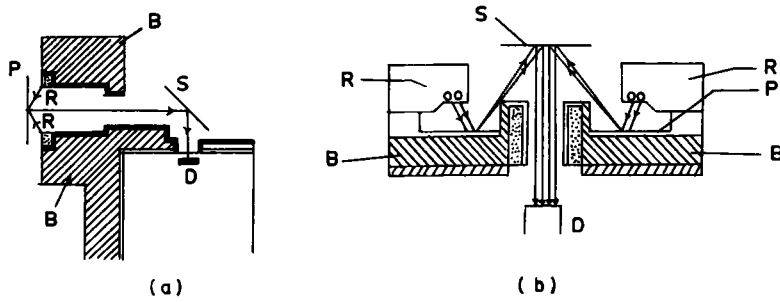


**Figure 1.** Schematic diagram of the experimental arrangements used (a) in the present measurements (b) by Garg *et al* (1986).

R – radioactive source  $^{241}\text{Am}$ ; P – primary target;  
 S – secondary target of Ho; D – Si(Li) X-ray detector;  
 B – shielding material.

the radiation emitted from the primary targets is collimated to fall on the secondary target of Ho. The *L*-shell fluorescent X-rays emitted from the Ho target are recorded with Si(Li) X-ray detector (D), with resolution of  $\sim 180\text{ eV}$  at  $5.9\text{ keV}$ , coupled to an ND-600 multi-channel analyser. The Si(Li) detector has a crystal active diameter of  $10\text{ mm}$ , a sensitive depth of  $4.66\text{ mm}$  with Be window of thickness  $0.0254\text{ mm}$ . The shielding in both the arrangements is so arranged that the source can only see the primary target. The primary and the secondary targets can see each other and the detector can receive radiation only from the secondary target. In the set-up shown in figure 1(b) used by Garg *et al* (1986), the conditions imposed on shielding necessitate the use of primary targets in the form of annular rings with tungsten shielding behind them to prevent direct entry of gamma rays from the source into the detector. The detector-secondary target distance has also to be relatively large since the detector has to be placed behind the primary target shielding. In our set-up, figure 1(a), self-supporting primary targets in the form of discs without any shielding behind them are used and the detector is placed close to the secondary target as compared to the earlier arrangement. A thin foil of  $\text{HoF}_3$  of thickness  $91\ \mu\text{g}/\text{cm}^2$  evaporated on a  $6.3\ \mu\text{m}$  thick mylar backing and self-supporting disc of  $\text{Ho}_2\text{O}_3$  of  $274\ \text{mg}/\text{cm}^2$  thickness and dia  $4\text{ cm}$  were used by Garg *et al* (1986) and the present authors respectively. The target was prepared by the method as described in Singh and Sood (1972). In one case, the target behaves as infinitely thin while in other as infinitely thick. In the former case, the effective thickness of the target is equal to its real thickness while in the latter case, it is equal to the reciprocal of the sum of the absorption coefficients of the incident and emergent X-rays in  $\text{Ho}_2\text{O}_3$  and is independent of the real thickness of the target. The absorption coefficients in the energy range of  $10$  to  $40\text{ keV}$  involved in the present measurements are well-known with an accuracy  $\sim 5\%$  but the measurement of absolute thickness of evaporated  $\text{HoF}_3$  layer on mylar backing involves subtraction of two small quantities with rather large errors. The percentage uniformity of thickness of these thin targets is expected to be lower than that of thick targets, moreover, more than  $99\%$  of X-rays of energy  $25\text{ keV}$  are transmitted through  $\text{HoF}_3$  foil without any interaction, thereby reducing signal to background ratio considerably. All these factors added to uncertainties in the final results obtained by Garg *et al* (1986). The strength of  $^{241}\text{Am}$  source used here is about three times that

used by Garg *et al* (1986). In the new measurement, the use of higher source strength alongwith infinitely thick  $\text{Ho}_2\text{O}_3$  target, a disc instead of annular ring primary target and smaller secondary target to detector distance reduces the time of measurement to  $\sim 20\%$ . Whereas Garg *et al* (1986) has not measured the  $L_1$  cross-sections due to poor counting statistics under the  $L_1$  peak in their set-up even for an observation time of 60,000 s, we were able to measure counts under  $L_1$  peak in 10,000 s in the new set-up with an accuracy of 2–3 per cent. The source to primary target, primary target to secondary target, secondary target to detector distances and shielding, for the measurement at each energy were so arranged that maximum signal to background ratio was obtained. In a typical case of Ag primary target, the distances were 0.6 cm, 8 cm and 2.5 cm respectively. In both the set-up, the radiation which falls on Ho target consist mainly of  $K$ ,  $L$  and higher shell fluorescent X-rays characteristic of the primary target elements and coherent and incoherent scattering of 59.57 keV gamma rays from the primary targets, the backing and shielding material behind them (if any). Since it is desired to measure the cross-sections for the production of  $L$  X-rays in Ho by the  $K$  conversion X-rays of the primary target elements, the experimental set-up and procedure used should enable the isolation and counting of these  $L$  X-rays of Ho which are produced only by the primary target  $K$  X-rays. With suitable choice of primary target elements, the energy of the primary  $L$  X-rays is kept lower than the  $L$ -shell threshold energy of Ho to eliminate the production of Ho  $L$  X-rays by primary target  $L$  and higher shell X-rays in our experiment and that of Garg *et al* (1986). However, the energy of gamma rays scattered coherently and incoherently from the primary targets are greater than the  $K$  and  $L$  threshold energies of Ho respectively. Therefore, while both  $K$  and  $L$  shell electrons of Ho are ionized by coherent scattering, only the  $L$  shell electrons are ionized by incoherent scattering and both produce additional unwanted Ho  $L$  X-rays. We have made an effort not only to reduce the unwanted contribution due to scattering by avoiding the need of any shielding material behind the primary target, but also to experimentally determine and properly subtract its contribution by using an equivalent Al primary target. The spectra of radiation emitted from the primary target element and an equivalent Al target are matched to give almost the same scattering by adjusting the thickness of the equivalent Al target. Typical results are shown in figure 2 where  $A$  and  $B$  represent the spectral distribution of radiation emitted from Zr and equivalent Al primary targets respectively. The scattering of 59.57 keV gamma rays is seen to be almost the same from both the targets. The  $C = A - B$  spectrum shown in figure 2(b) consists almost entirely of  $K$  conversion X-rays of Zr. Thus the conditions are so arranged that the Ho  $L$  X-rays which are produced only by the interaction of  $K$  conversion X-rays of primary targets with  $L$  shell electrons of Ho are counted. Garg *et al* (1986) have not reported the spectral distribution of radiation which actually falls on their  $\text{HoF}_3$  target and excites  $L$  shell X-rays in it. The spectral distribution of radiation emitted from Ho when it is irradiated, in turn, with radiation from primary targets of Zr and equivalent Al is shown in figure 3(a), by  $D$  and  $E$ . The part of the spectrum  $F = D - E$  between channels from 50 to 140 corresponds to  $L$  X-rays of Ho produced only by the interaction of the  $K$  conversion X-rays of Zr with  $L$  shell electrons of Ho. Complete match of spectra  $D$  and  $E$  between channels 700 to 1000 shows that the contribution of scattering from the experimental and equivalent Al primary targets is almost the same. From the comparison of spectra  $D$  and  $E$ , it is seen that the additional contribution to  $L$  X-rays of Ho due to scattering from primary target of Zr is  $\sim 25\%$ .

Assuming isotropic emission of X-rays, the cross-section for the production of Li group of secondary L X-rays by the primary K conversion X-rays is given by

$$\sigma_{L_i}^{\bar{x}} = N_{L_i} \frac{M_L}{N} \cdot \frac{1}{2 t_L \beta_{L_i}} [4\pi / I_0 \omega \epsilon_{L_i}] \quad (1)$$

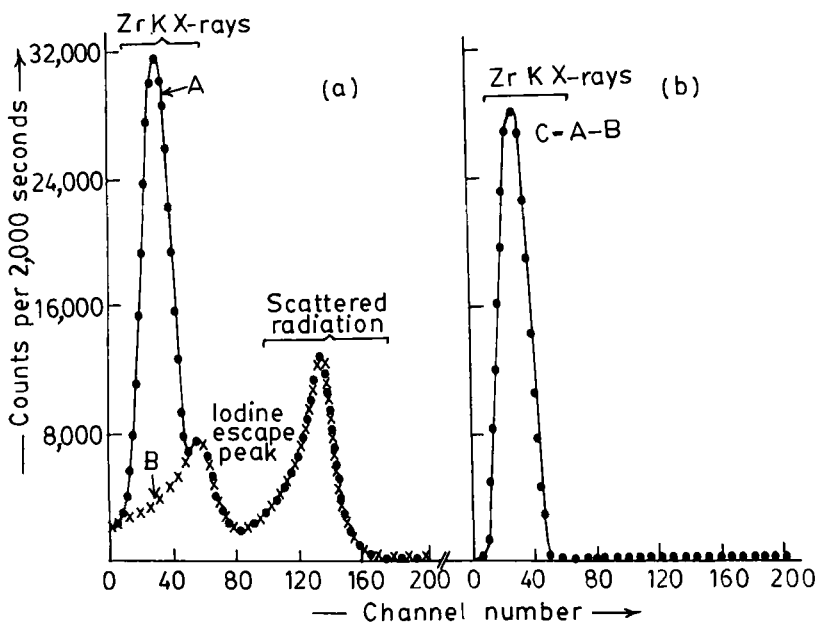
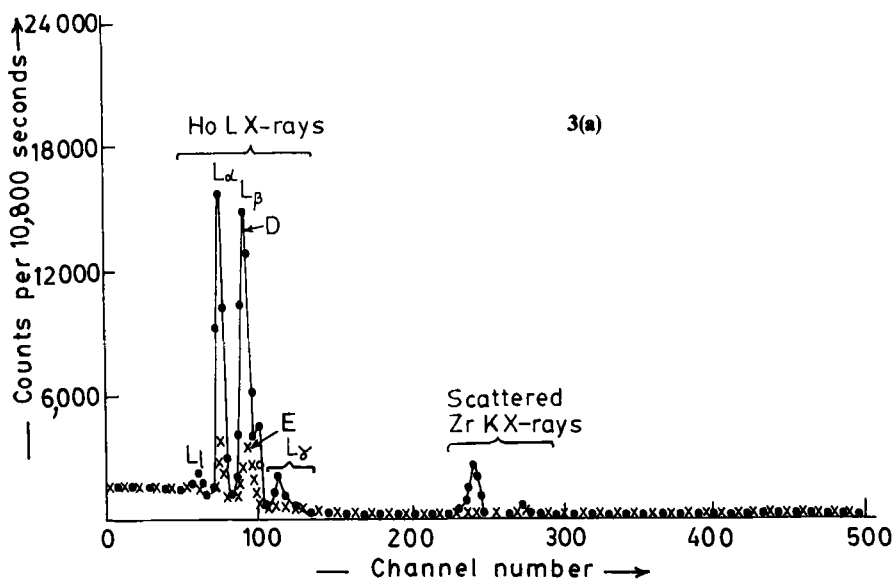


Figure 2. Primary spectra recorded with 2" dia and 0.04" thick NaI(Tl) crystal spectrometer placed at secondary target (Ho) position when the primary targets were irradiated with 59-57 keV gamma rays from  $^{241}\text{Am}$ . (a) A, Zr - primary; B - equivalent Al primary. The first intense peak is due to Zr K X-rays and the second peak is due to the scattered radiation, (b) C = A - B.



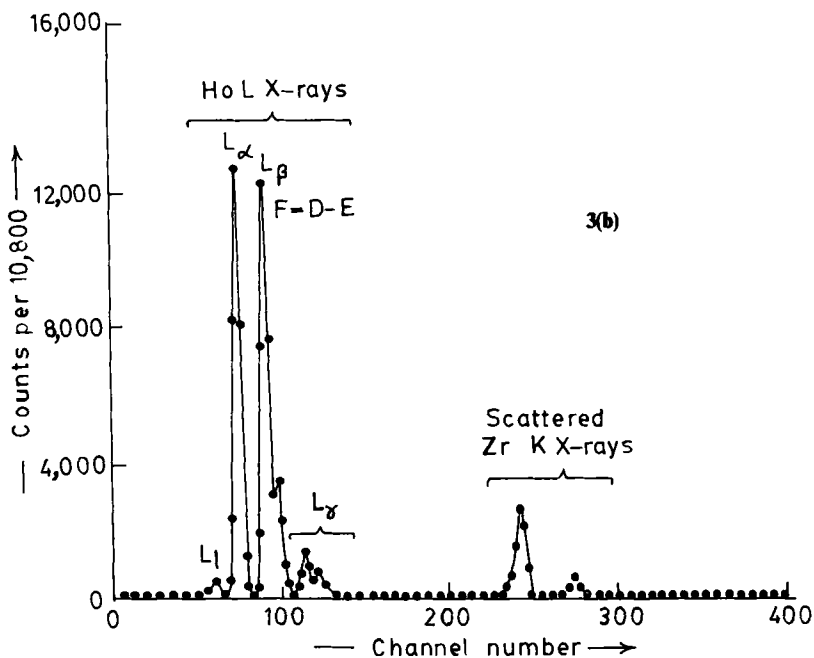
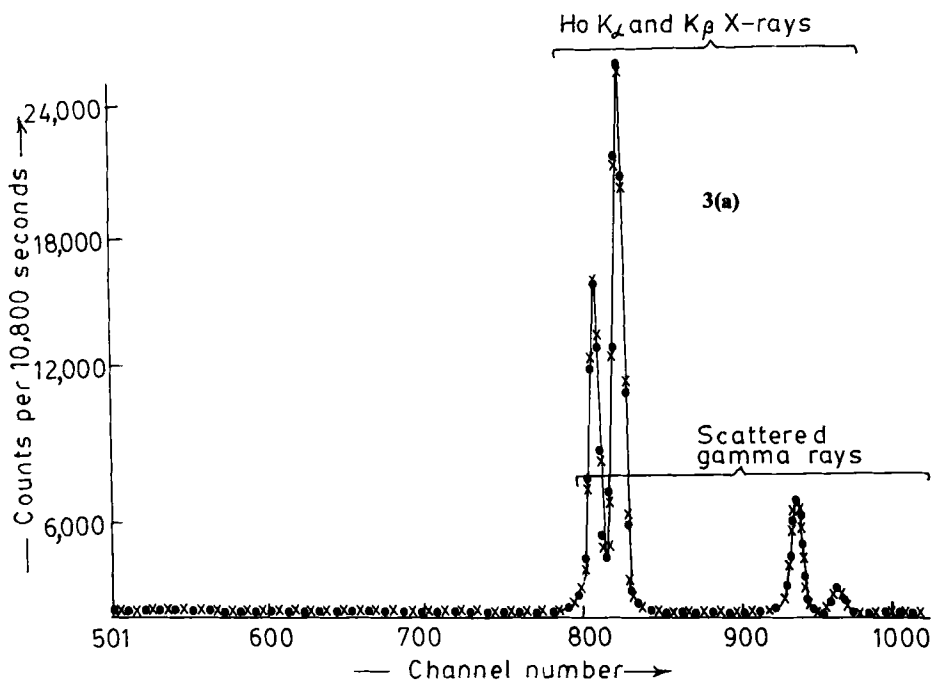


Figure 3. Secondary target spectra recorded with Si(Li) X-ray detector. (a) D-Zr primary and Ho secondary; E-equivalent Al primary and Ho secondary, (b) F = D - E.

where  $N_{L_i}$  is the number of Ho  $L$  X-rays counted per unit time under the peak due to  $L_i$  group by the spectrometer;  $I_0$  is the number of primary K conversion X-rays falling on the  $\text{Ho}_2\text{O}_3$  target per unit time;  $M_L$  is the molecular weight of  $\text{Ho}_2\text{O}_3$ ;  $N$  is Avogadro number;  $\omega$  is the solid angle subtended by the  $\text{Ho}_2\text{O}_3$  target on the detector;  $\varepsilon_{L_i}$  is the detector efficiency of the spectrometer under the peak  $L_i$ ;  $t_L$  is thickness of the  $\text{Ho}_2\text{O}_3$  target;  $\beta_{L_i}$  is the self-absorption correction factor of the  $\text{Ho}_2\text{O}_3$  target which accounts for the absorption of the incident and emitted X-rays in the target and it is expressed in terms of the known values of the absorption coefficients for the incident  $\mu_i$  and emitted  $\mu_e$  X-rays as:

$$\beta_{L_i} = \frac{1 - \exp[-(\mu_i + \mu_e)t_L/\cos\theta]}{(\mu_i + \mu_e)t_L/\cos\theta} \quad (2)$$

In the present measurement  $\theta = 45^\circ$  and the target is infinitely thick, therefore, effective thickness which is the product of real thickness  $t_L$  and the correction factor  $\beta_{L_i}$  approaches  $[1/(\mu_i + \mu_e)\sqrt{2}]$  whereas in the experiment of Garg *et al* (1986) the target is infinitely thin and the effective thickness approaches the real thickness.

The values of  $N_{L_i}$  were determined from the areas under the  $L_i$ ,  $L_\alpha$ ,  $L_\beta$  and  $L_\gamma$  X-ray peaks. Sufficient number of runs were taken to achieve a statistical accuracy of  $\sim 1\%$  in the counting rates. The values of the effective thickness,  $\beta_{L_i}t_L$  were calculated using the semi-empirical values of absorption coefficients from the tables of Veigele (1973) as explained earlier (Arora *et al* 1981). The values of the factor  $[4\pi/I_0\omega\varepsilon_{L_i}]$  which contains terms relating to the flux of primary K conversion X-rays falling on the  $\text{Ho}_2\text{O}_3$  target, geometry factor and absolute efficiency of the X-ray detector were determined in a separate experiment. For this purpose, secondary targets having the same diameter as  $\text{Ho}_2\text{O}_3$  target and of elements, Ti, Fe, Ni, Cu, Zn, Ge and Se whose K X-ray energies lies in the range of 4–12 keV were irradiated, in turn, with K conversion X-rays of all the primary target elements, as used in the main experiment and the intensity of the K-shell X-rays emitted in each case was measured

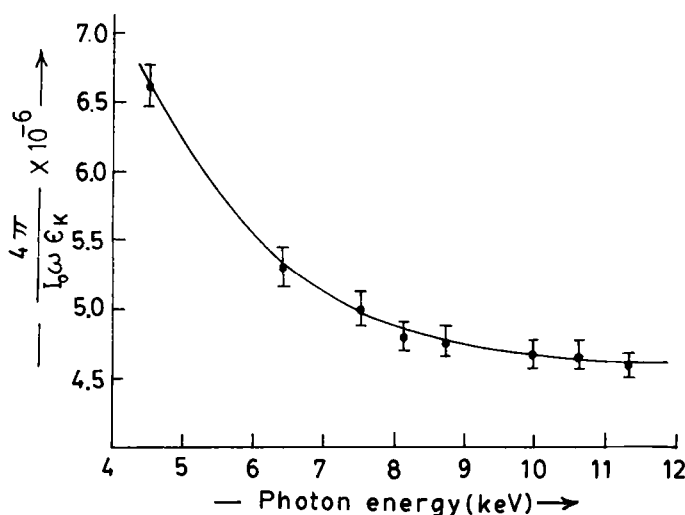


Figure 4. Plot of  $[4\pi/I_0\omega\varepsilon_K]$  vs photon energy.

with the same spectrometer as used for the measurement of Ho L X-rays. The number of K X-ray  $N_K$  emitted from a target per unit time are given by a relation similar to expression (1) as above which may be written as:

$$\frac{4\pi}{I_0\omega\varepsilon_K} = \frac{\sigma_K^x N t_K \beta_K}{N_K M_K} \quad (3)$$

All the terms of (3) have the same meaning as discussed (1), but subscript K indicates that these terms correspond to K-shell.

Using measured values of  $N_K$  and from the knowledge of  $\sigma_K^x$  and other parameters of the targets, the values of the term  $[4\pi/I_0\omega\varepsilon_K]$  were determined at weighted mean K X-ray energies of elements  $22 \leq Z \leq 34$  and plotted against energy as shown in figure 4. The values of this term at  $L_i$ ,  $L_\alpha$ ,  $L_\beta$ , and  $L_\gamma$  X-ray energies of Ho were read from the graph to calculate the values of the cross-sections  $\sigma_{L_i}^x$ ,  $\sigma_{L_\alpha}^x$ ,  $\sigma_{L_\beta}^x$ , and  $\sigma_{L_\gamma}^x$  from (1).

### 3. Results and discussion

The measured values of the cross-sections for the production of  $L_i$ ,  $L_\alpha$ ,  $L_\beta$ , and  $L_\gamma$  groups of L-subshell X-rays of Ho by photons of energies 10.005, 11.372, 13.596, 16.035, 17.781, 22.581, 25.77, 32.89 and 38.189 keV are compared with other available experimental (Garg *et al* 1986) and calculated values (Table 1). The calculated values are determined from the theoretical values of L-subshell photoionization cross-sections (Scofield 1973), radiative decay rates (Scofield 1974), and semi-empirically fitted values of fluorescence yields and Coster-Kronig transition probabilities (Krause *et al* 1979) using the following relations:

$$\begin{aligned} \sigma_{L_i}^x &= [\sigma_{L_1}(f_{13} + f_{12}f_{23}) + \sigma_{L_2}f_{23} + \sigma_{L_3}] \omega_3 F_{3i} \\ \sigma_{L_\alpha}^x &= [\sigma_{L_1}(f_{13} + f_{12}f_{23}) + \sigma_{L_2}f_{23} + \sigma_{L_3}] \omega_3 F_{3\alpha} \\ \sigma_{L_\beta}^x &= \sigma_{L_1} \omega_1 F_{1\beta} + (\sigma_{L_1}f_{12} + \sigma_{L_2}) \omega_2 F_{2\beta} \\ &\quad + [\sigma_{L_1}(f_{13} + f_{12}f_{23}) + \sigma_{L_2}f_{23} + \sigma_{L_3}] \omega_3 F_{3\beta} \\ \sigma_{L_\gamma}^x &= \sigma_{L_1} \omega_1 F_{1\gamma} + (\sigma_{L_1}f_{12} + \sigma_{L_2}) \omega_2 F_{2\gamma} \end{aligned}$$

where  $\sigma_{L_1}$ ,  $\sigma_{L_2}$  and  $\sigma_{L_3}$  are L-subshell photoionization cross-sections at the experimental energies;  $\omega_1$ ,  $\omega_2$  and  $\omega_3$  are L-subshell fluorescence yields;  $f_{12}$ ,  $f_{13}$  and  $f_{23}$  are the Coster-Kronig transition probabilities;  $F$ 's are the fractional radiative decay rates and  $F_{3i}$  is the fraction of  $L_3$  subshell X-rays which contribute to the  $L_i$  peak of the X-ray spectrum of Ho. All other  $F$ 's are similarly defined. The errors in the present measurements are  $\sim 5-7\%$  which are due to the counting statistics and the uncertainties involved in the determination of other parameters used for the determination of the cross-sections from (1). The cross-sections at some of the energies were again measured, after about six months by different workers. The results of the two independent experiments were found to agree with each other within the experimental uncertainties showing that the present results do not involve any serious systematic errors. The results of the measurement at 22.6 keV (Mann *et al* 1990a) are also listed in table 1 for illustration.

Table 1. The measured values of  $\sigma_{L_i}^x$ ,  $\sigma_{L_i}^y$ ,  $\sigma_{L_i}^z$  and  $\sigma_{L_i}^x$  (in b/a) compared with the available experimental and the calculated values.

Excitation energy (keV)	Experimental	Calculated	Experimental	Calculated	Experimental	Calculated	Experimental	Calculated
10-005	250 ± 15	249	5700 ± 300	5880	5290 ± 270	5220	**	84
11-372	171 ± 12	175	4100 ± 225	4130	3700 ± 215	3800	625 ± 43	623
13-596	109 ± 8	107	5049 ± 297*	2535	4855 ± 286*	2450	641 ± 46*	441
16-035	70 ± 5	68	2566 ± 155	1610	2460 ± 155	1625	410 ± 28	278
17-781	53 ± 4	51	1610 ± 92	1205	1600 ± 90	1245	267 ± 18	216
22-581	23 ± 2	26	1230 ± 65	607	1250 ± 62	670	215 ± 18	119
25-77	24 ± 2.5***	17.5	1266 ± 58*	415	1327 ± 58*	475	223 ± 12*	86
32-89	8 ± 0.6	8.6	596 ± 38	205	643 ± 43	249	120 ± 7	46
38-184	6 ± 0.4	5.6	710 ± 44*	133	751 ± 46*	168	143 ± 9*	32
			595 ± 36***		683 ± 40***		113 ± 9***	
			395 ± 25		455 ± 28		78 ± 6	
			482 ± 27*		577 ± 32*		96 ± 6*	
			202 ± 12		250 ± 13		45 ± 3	
			131 ± 8		163 ± 8		30 ± 2	

\* Indicates the measured values of cross-sections by Garg et al (1986)

\*\* Indicates that  $L_{\gamma}$  cross-sections for Ho at 10-005 keV could not be measured as the scattered fluorescent K X-rays of Ge overlap with the L X-rays.

\*\*\* Indicates the experimental values of the cross-sections measured in an independent experiment by the authors at different times.

It is evident from table 1 that our values are consistently lower than those of Garg *et al* (1986) but agree with the theory and do not show any systematic regular trends which would indicate any definite departure from theory. The higher values obtained by Garg *et al* (1986) are most probably due to an over-estimation of the Ho *L* X-rays. In their method of measurement, Garg *et al* (1986) have not isolated Ho *L* X-rays which are produced by the interaction of primary target *K* conversion X-rays with *L*-shell electrons of Ho from those *L* X-rays of Ho which are produced by the coherently and incoherently scattered gamma-rays from primary targets to determine cross-sections for the production of Ho *L* X-rays by the primary *K* conversion X-rays. The additional contribution to the measured yield of *L* X-rays of Ho by gamma ray scattering from primary targets will result in higher values of measured cross-sections. Garg *et al* (1986) have not reported the spectrum of radiation actually falling on Ho target in their experiment which in our opinion is very important to confirm that no radiation other than that of the desired energy is responsible for the production of *L* X-rays of Ho. Any admixture of impurity in radiation falling on Ho target and capable of exciting *L* X-ray in it, will yield higher values of measured cross-sections. The gamma rays falling on Ho target after scattering from primary target and shielding behind it will have sufficient energy to excite both the *K* and *L* shell electrons of Ho. Most of the vacancies in the *K* shell are also transferred to the *L*-shell and contribute to additional *L* X-rays. While the additional contribution to the production of *L* X-rays of Ho by the scattering from target has been experimentally determined and subtracted by us, it has not been accounted for in the measurements of Garg *et al* (1986) thereby yielding higher values of measured cross-sections.

We observed (Singh *et al* 1987) that the higher values of cross-sections measured by Garg *et al* (1986) are due to the unwanted contribution to the production of *L* shell X-rays in secondary targets by gamma rays scattered from the primary targets. Garg *et al* estimated this additional contribution due to the ionization of *K* and *L* shell electrons of the secondary target by scattered gamma rays to be of the order of 4–10% and 4% respectively and reported (Singh *et al* 1989) revised measurements of cross-sections for some elements and photon energies. The revised values of cross-sections for Ho are, however, not available for comparison with the present measurements.

It may be pointed out that one has to carefully measure the integral cross-sections for the emission of  $L_i$  and  $L_\alpha$  groups of *L* X-ray lines, in view of the spatial anisotropic emission of these groups of lines recently observed by us (Kahlon *et al* 1990a). The differential cross-sections for the emission of  $L_i$  and  $L_\alpha$  groups of X-ray lines produced in Pb, Th and U by 60 keV photons are found to decrease consistently when the X-ray emission angle varies from 40° to 120° (Kahlon *et al* 1990b, 1991). However, a fairly good agreement of our present measurements with theory may be due to the reason that for the X-ray emission from Ho either the anisotropy is small or its effects at angles smaller and greater than 90°, compensate one another.

### **Acknowledgement**

The financial assistance from the DST, Govt. of India and UGC is gratefully acknowledged.

**References**

- Arora S K, Allawadhi K L and Sood B S 1981 *J. Phys.* **B14** 1423
- Garg M L, Mehta D, Verma H R, Singh Nirmal, Mangal P C and Trehan P N 1986 *J. Phys.* **B19** 1615
- Kahlon K S, Shatendra K, Allawadhi K L and Sood B S 1990a *Pramana – J. Phys.* **35** 105
- Kahlon K S, Aulakh H S, Singh N, Mittal R, Allawadhi K L and Sood B S 1990b *J. Phys.* **B23** 2733
- Kahlon K S, Aulakh H S, Singh N, Mittal R, Allawadhi K L and Sood B S 1991 *Phys. Rev.* **A43** 1455
- Krause M O, Nestor C W Jr, Spark C J Jr and Ricci E 1979 *J. Phys. Chem. Ref. Data.* **8** 307
- Mann K S, Singh N, Mittal R, Allawadhi K L and Sood B S 1990a *J. Phys.* **B23** 2497
- Mann K S, Singh N, Mittal R, Allawadhi K L and Sood B S 1990b *J. Phys.* **B23** 3521
- Scofield J H 1973 Lawrence Livermore Laboratory Report No. IJCRL-51326
- Scofield J H 1974 *Atomic Data Nucl. Data Tables* **14** 121
- Singh M J and Sood B S 1972 *Nuovo Cimento* **88** 261
- Singh N, Mittal Raj, Allawadhi K L and Sood B S 1987 *J. Phys.* **B20** 5639
- Singh S, Mehta D, Kumar S, Garg M L, Singh Nirmal, Mangal P C and Trehan P N 1989 *X-ray Spectrometry* **18** 193
- Viegele Wm J 1973 *At. Data Tables* **5** 51